Robotica (2004) volume 22, pp. 493–503. © 2004 Cambridge University Press
DOI: 10.1017/S0263574704000244 Printed in the United Kingdom

A controllability criterion based on a physical analogy: Limbless locomotion and Object grasping in Robotics

Zeki Y. Bayraktaroglu* and Pierre Blazevic†

(Received in Final Form: January 12, 2004)

SUMMARY
This paper deals with the controllability of biologically inspired snake-like mechanisms. Motion equations of the generic snake-like mechanism and investigations on its controllability lead to extremely complicated mathematical representations. The authors establish a physical analogy between the undulatory snake locomotion and object grasping. Based on this analogy, they propose a controllability criterion concerning the motion of the mobile mechanism. Results of dynamic simulations of the controlled system systematically point to the validity of the analogy-based controllability criterion. The purpose of this work is to achieve an understanding of the undulatory motion which constitutes the basis of a biologically motivated experimental setup.

KEYWORDS: Controllability; Grasping; Limbless locomotion; Mobile robots, Snake-like mechanisms; Physical analogy.

1. INTRODUCTION

In our previous research on terrestrial limbless locomotion[1] we proposed a class of novel planar mechanisms, i.e. *Snaca-N*, dedicated to imitate one type of natural snake motion, namely the lateral undulation. *Snaca-N* was a biologically inspired planar locomotor model that gave rise to extremely complicated motion equations. Two coupled mechanical actions, both of them simultaneously required for the locomotion to take place, were at the heart of the problem. In this very first approach, we failed to find out a proper motion control scheme for the system constituted by the mobile mechanism and its environment. In the second part, we shall present the original mechanism and the related problem statement.

Snaca-N's mechanical structure was then reviewed in order to overcome the above mentioned mathematical complexity. Modification of the original structure allowed us to decouple the two mechanical actions and avoid any model-based control approach. The third part will present the modified mechanism and redefine the control problem.

However, we were not able to derive definite conclusions on the controllability of our newly defined system. At this stage, a physical analogy between the limbless locomotion by lateral undulation and the grasping in robotics was established, and we succeeded to propose a kind of novel controllability criterion for the locomotion of *Snaca-N* by lateral undulation. In the fourth part, we shall overview the grasping, as studied in robotics, and present our controllability criterion based on a physical analogy.

Dynamic simulations of the controlled system were finally realized. Simulation results systematically points out the validity of our controllability criterion. In the fifth part, we shall discuss the actual results and present some future prospects of this work.

2. LIMBLESS LOCOMOTION THROUGH LATERAL UNDULATION

2.1. Related work

In our previous works[1,2] we have studied the natural limbless locomotion exerted by terrestrial snakes. We were particularly interested in lateral undulation, the typical mode of snake-like locomotion. Research concerning natural snake locomotion and snake-like robotic locomotion can be found in the works of Gray,[3,4] Jayne,[5] McNeill,[6] Gasc,[7] Renous,[8] Kelley, Arnold and Gladstone,[9] Hirose,[10] Mori and Hirose,[11] Burdick et al.,[12] Chirikjian,[13,14] Chirikjian and Burdick,[15] Ostrowski,[16] Dowling,[17] Klaassen and Paap,[18] and Miller[19] among others. In this section, we shall present the generic planar mobile mechanism dedicated to exercise lateral undulation in a given environment and investigate its features of controllability.

The mechanism shown in Fig. 1 is a planar chain consisting of identical rigid bodies. Each joint between successive links is given one DOF, namely a rotation around the vertical axis. We assume that revolute joint actuators generate the rotational motions. This is a basic discrete model of the natural snake body. In the literature, such mechanical structures are known as *non-holonomic Caplygin* systems.[20] Various researches on the motion control of this kind of articulated mechanisms are presented by Sreenath,[21] Sreenath et al.,[22] Reyhanoglu and McClamroch,[23–25] Yang,[26] De Luca and Oriolo.[27]

One of the main application areas appears to be the orientation control, i.e. the reorientation of satellites in orbit around the world. Local controllability of this kind of

* Istanbul Technical University (ITU), Faculty of Mechanical Engineering, System Dynamics & Control Department, Inonu Caddesi No. 87, Gumussuyu 34439, Beyoglu Istanbul (Turkey).
E-mail: zeki.bayraktaroglu@itu.edu.tr *(Corresponding author).
† Université de Versailles Saint Quentin-en-Yvelines (UVSQ), Laboratoire de Robotique de Versailles (LRV), 10-12 avenue de l'Europe, 78140 Vélizy-Villacoublay (France).
E-mail: pierre.blazevic@robot.uvsq.fr

https://doi.org/10.1017/S0263574704000244 Published online by Cambridge University Press

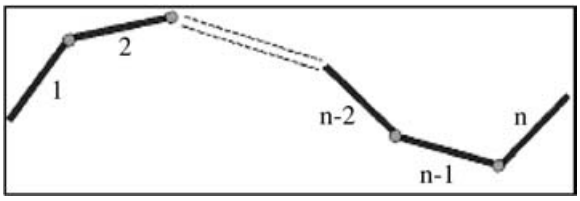


Fig. 1. The generic planar snake-like mechanism: Snaca-N.

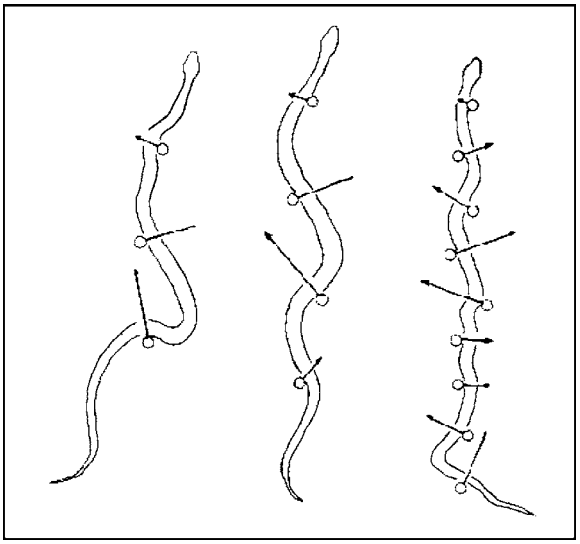


Fig. 2. Illustration of a snake in lateral undulation with various numbers of push-points.

articulated system using only internal actions has been proved and tested through simulations.[23] We recall that in these works, the mentioned local controllability concerns only a limited number of output variables, such as the orientation of a single link with respect to a given reference frame. The motion of a multi-body satellite in orbit is subject to the law of conservation of angular momentum and therefore is analogous to the motion of the famous falling cat.

On the other hand, locomotion through lateral undulation can be achieved if and only if the snake or any articulated snake-like mobile mechanism, e.g. *Snaca-N*, laterally interacts with the environment. The minimal number of required simultaneous lateral contacts is known to be 3 for snakes exercising lateral undulation. This number has been experimentally determined by Gans[28] who observed snakes in motion, and Gasc also pointed out the same number. In the following sections, we shall redefine this required minimal number p with respect to the mechanical properties of contacts between the mobile body and its environment.

Figs. 2 and 3 illustrate, respectively, the generation of lateral propulsive forces required for locomotion of snakes and of *Snaca-N*. The mechanism is expected to push against discrete push-points whose positions are fixed with respect to a reference frame. Reaction forces from these simultaneous contacts constitute the propulsive force for the mobile body. In lateral undulation, each link of the mobile mechanism faithfully follows the path taken by the leading link. The entire mechanism slides over the ground by maintaining its lateral contacts with the considered push-points.

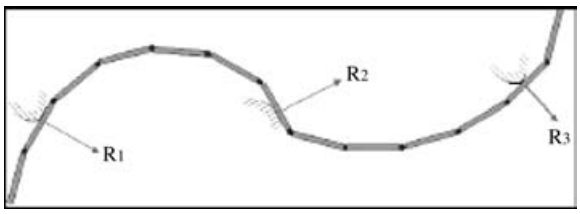


Fig. 3. 3 simultaneous push-point reactions required for the propulsion of the Snaca-13.

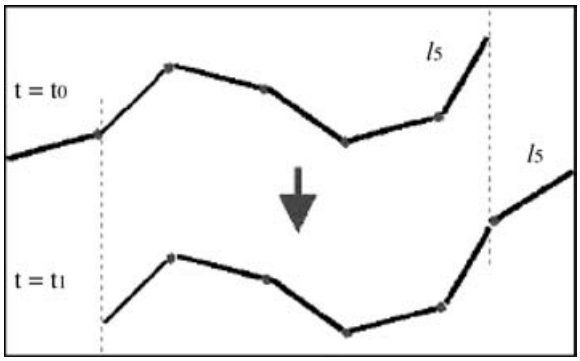


Fig. 4. Initial and final configurations of the Snaca-6 in a progression step.

2.2. *Modeling*

Definition 1. Let l_i be the ith link of Snaca-N and t_0 be an arbitrary initial moment in its undulatory motion. A *progression step* corresponds to the time interval from t_0 to t_1, during which the links l_i (with $i = 1 \ldots N-1$) of the chain move to reach at t_1 the positions and orientations of the links l_{i+1} at the initial moment t_0. The leading link l_N follows an independent trajectory from the rest of the mechanism.

The above definition results from our biologically inspired approach to the problem in the sense where each section of the snake's body faithfully follows the path taken by the head. Succession of progression steps should give rise to the desired undulatory progression motion. Therefore the progression step can be considered as the fundamental progressive motion of the locomotion by lateral undulation. In this work, we shall study the motion of *Snaca-N* during one progression step. A progression step of a six-link mechanism is illustrated in Fig. 4.

At this stage, we assume that link/push-point interactions can be modeled by spring/dampers associated to the ground/push-point connections, as illustrated in Fig. 5. Under this assumption, force control at contact levels is reduced to position control of the mobile links with respect to the fixed positions of the push-points. In order to control the motion of *Snaca-N* in a desired trajectory, one needs to coordinate the reconfiguration of the internal shape and the generation of the lateral forces to be applied against available push-points.

The internal shape is determined by the joint positions. Since the mechanism can be instantaneously considered as a rigid body, position and orientation of a single link in a fixed reference frame are sufficient to determine the mechanism's absolute coordinates in this same frame. The state of *Snaca-N* in the reference frame in terms of positions

https://doi.org/10.1017/S0263574704000244 Published online by Cambridge University Press

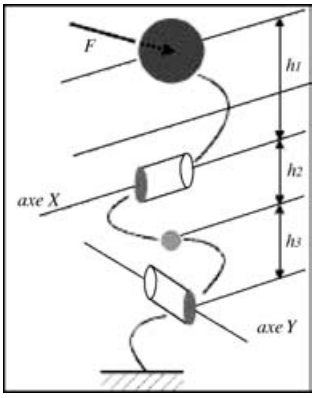


Fig. 5. Push-point model.

is given by:

$$\underline{X}_r = [x_r, y_r, \theta_r]^T \tag{1}$$

$$\underline{\psi} = [\psi_1, \psi_2, \ldots, \psi_{n-1}]^T \tag{2}$$

where $\underline{X}_r$ defines the absolute position and orientation of one of the mechanism's links (arbitrarily chosen *cyclic coordinates* of the system) and $\underline{\psi}$ is the vector of joint positions. $\underline{X}_r$ and $\underline{\psi}$ together represent the generalized variables for an instantaneous configuration of the mechanism.

Remark 1. (1) and (2) happen to be $n + 2$ output variables of the system. The input vector consists of $n - 1$ elements, namely the velocities or torque of $n - 1$ joint actuators. Hence the system is underactuated and is not globally controllable for the reconfiguration of the entire mechanism.

We define desired trajectories to be followed for each link in a given progression step. Let

$$\underline{\Psi}_1 = \left[\underline{X}^1_{rd}, \underline{\psi}^1_d\right]^T \tag{3}$$

represent the desired link trajectories for a given progression step.

On the other hand, generation of required lateral forces depends on the positions and orientations of the links with respect to the fixed push-points in the reference frame. Therefore one needs another set of desired instantaneous positions and orientations for the links interacting with lateral push-points:

$$\underline{\Psi}_2 = \left[\underline{X}^2_{rd}, \underline{\psi}^2_d\right]^T \tag{4}$$

Remark 2. Two distinct desired vectors (3) and (4) together constitute the desired state of the system. This coupling between two mechanical actions (the *internal* and *pushing* actions) propelling the system leads to highly complicated mathematical representations of the system dynamics. Furthermore, the system is not controllable for the desire task. Motion equations of the system developed through various approaches, such as *Lagrangian* and *non-canonical Hamiltonian*, happen to be highly complicated.[1]

In the next section, we shall present a modified structure of *Snaca-N*, which will rather be a control-oriented model.

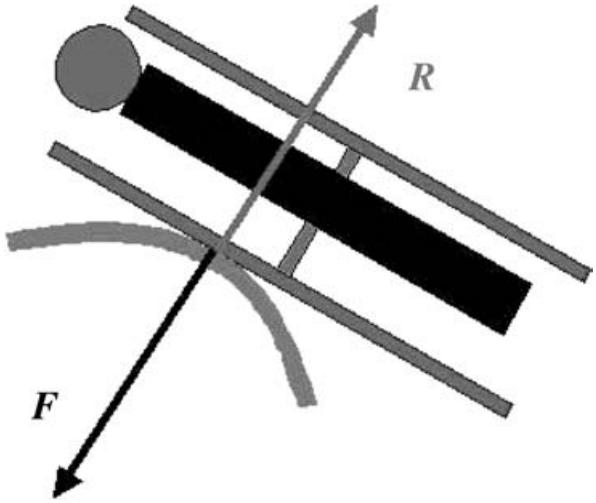


Fig. 6. One link of the modified Snaca-N pushing against a push-point, where $\vec{F}$ and $\vec{R}$ illustrate the applied and reaction forces.

3. THE MODIFIED SNACA-N AND THE FINAL PROBLEM STATEMENT

Fig. 6 represents one link of the modified mechanical structure of *Snaca-N*. Lateral thin plates mounted on each side of the links are driven through linear actuators and are expected to push against available push-points. This modification of the basic chain (Fig. 3) appears to complicate the mechanism. In fact, the system has been decoupled by this way therefore the internal and pushing actions can be realized independently from each other. Since we assume that the mechanism can reconfigure its shape and apply required forces to the push-points, any kinematic or dynamic model that should be involved in an eventual model-based control scheme will be avoided.

One can distinguish two different states of our mechanism with respect to its established contacts with available push-points. In any given configuration of *Snaca-N*, application of a force against a push-point is possible if and only if the considered pushing link is in a certain proximity of an available push-point. This upper limit for the link/push-point distance is determined by the lateral aperture of the thin plates. In our following study, we shall assume that the mechanism's links are close enough to the environment's push-points.

With the above-defined *Snaca-N*, the problem of motion control for progression by lateral undulation is reduced to the computation of required lateral forces to be applied to the environment's push-points. In this context, one needs to answer the following questions:

(i) Can *Snaca-N* (in an arbitrarily given internal configuration and in simultaneous lateral contacts with a finite number of push-points) move and progress by exerting the lateral undulation?
(ii) If so, what is this finite number of simultaneous lateral contacts?

The above questions deal with the conditions to be fulfilled for the controllability of the system. In the next section, we shall establish a physical analogy between the lateral undulation and grasping in order to answer these questions.

https://doi.org/10.1017/S0263574704000244 Published online by Cambridge University Press

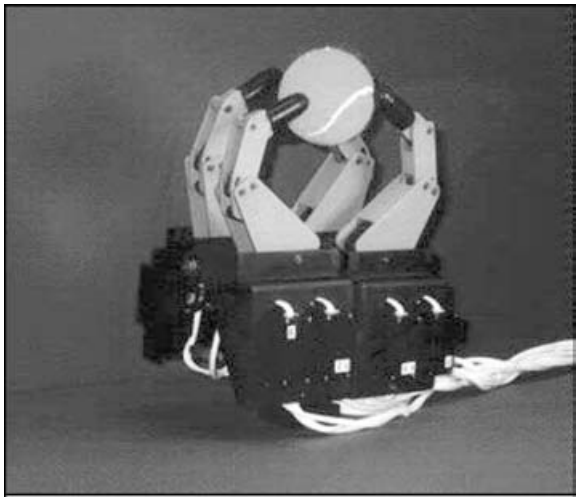


Fig. 7. Goldfinger (Clemson University).

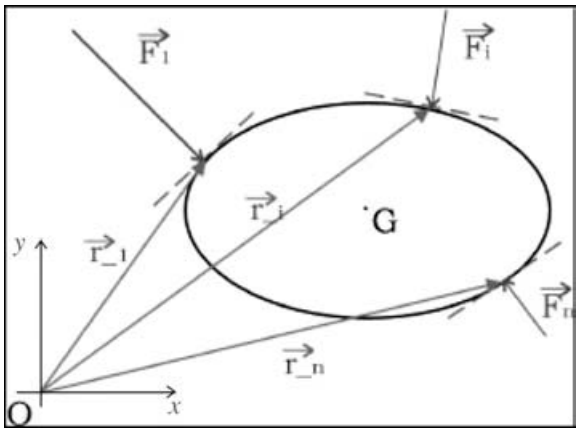


Fig. 8. An object gripped through 3 point contacts.

4. PHYSICAL ANALOGY BETWEEN GRASPING AND LATERAL UNDULATION

4.1. Grasping

In this section, we shall present some mathematical results on grasping[29–31] whose application area is generally object manipulation (displacement and/or reorientation) through multi-finger end-effectors of robot manipulators (Fig. 7). Stabilization of the gripped object is the main problem studied in grasping.

We assume that there is no static friction between the surface of the object and the fingers. Such non-frictional grips are called *positive grips*. We also assume point contacts between object surface and fingers. Hence a finger can apply only one force on the object along the surface normal at the point contact, directed inward. Fig. 8 illustrates the exterior forces applied to a rigid body through 3 simultaneous point contacts. If the geometry of the gripped object is known then the problem of grasping reduces to that of determining the following parameters:

(a) The position vectors $\underline{r}_1, \underline{r}_2, \ldots, \underline{r}_l; \underline{r}_i$ corresponds to the position of the object K at which the i^{th} finger makes contact with the object.

(b) The magnitudes of the forces $\underline{\alpha}_1, \underline{\alpha}_2, \ldots, \underline{\alpha}_l; \alpha_i$ corresponds to the magnitude of the force applied by the i^{th} finger along the unit surface normal $\underline{n}(\underline{r}_i)$ of the object at $\underline{r}_i$, directed inward. Since the forces must be unisense, α_i must be non-negative.

These parameters must satisfy the following conditions of equilibrium:

$$\begin{cases} \underline{F} + \sum_{i=1}^{l} \alpha_i \cdot \underline{n}(\underline{r}_i) = \underline{0} \\ \underline{\tau} + \sum_{i=1}^{l} \underline{r}_i \times \alpha_i \cdot \underline{n}(\underline{r}_i) = \underline{0} \end{cases} \tag{5}$$

where $\underline{F}$ and $\underline{\tau}$ represent, respectively, the exterior forces and torque applied to the gripped object. All the vectors are expressed in an arbitrarily fixed reference frame. The following questions arise in this context:

(i) Can an arbitrary object be gripped positively with a finite number of fingers?
(ii) If so, what are the grip points and force targets for such a grip?

These questions find their answers in a theorem where the following assumptions are satisfied:

Assumption 1. Each finger can be positioned accurately, subject to only a small deviation due to a lumped compliance between the finger top and bottom.

Assumption 2. The object K to be gripped is a closed bounded connected domain in two- or three-dimensional space and has a piecewise smooth boundary Σ.

Assumption 3. Each finger can apply only a single pure force, normal to surface through a frictionless point contact.

We now define the exceptional surfaces and force/torque closure grasp before introducing the existence theorem.

Definition 2. Let Σ be the boundary of an object K, where K is two-dimensional (respectively three-dimensional). Σ is said to be an *exceptional surface* if for some force/torque vector $\underline{g} = [\underline{F}, \underline{\tau}]$ in $\Re^3$ (respectively in $\Re^6$) the following property holds:

At each point $\underline{r}$ on Σ, the normal $\underline{n}(\underline{r})$ at $\underline{r}$ is perpendicular to $\underline{F} + \underline{\tau} \times \underline{r}$.

In other words, the boundary of an object is said to be exceptional if it is not possible to positively grip this object. The boundary of a sphere is an example to exceptional surfaces. Any set of external forces applied to a sphere gives zero torque with respect to its mass centre. Therefore, a non-null exterior torque cannot be balanced whatever the number of frictionless point contacts.

Definition 3. A set of gripping points on an object K is said to constitute a *force/torque closure grasp* if and only if arbitrary external force/torque acting on object K can be balanced by pressing the fingertips against this object at the selected grip points.

Theorem 1.[29] Let K be an object with boundary Σ, where K satisfies the assumptions 1, 2 and 3. Then

https://doi.org/10.1017/S0263574704000244 Published online by Cambridge University Press

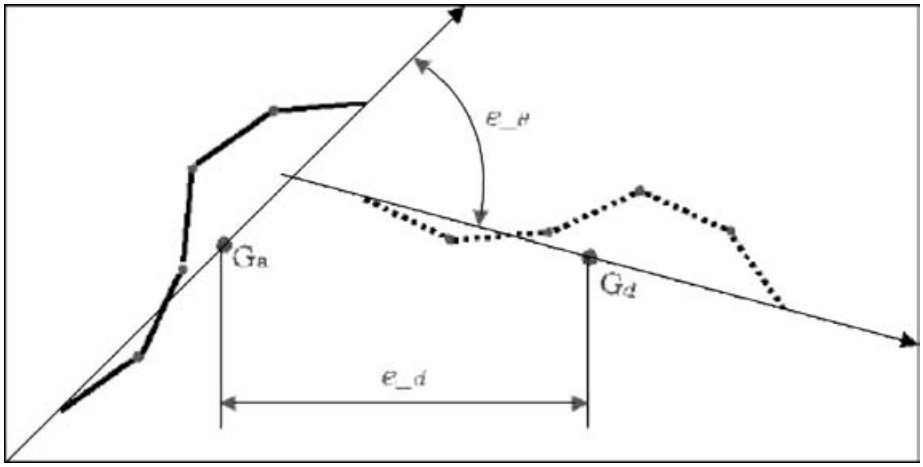


Fig. 9. The Snaca-5 in motion, considered instantaneously as a rigid body.

(a) K can be held at equilibrium by a positive grip of $m \leq k+1$ fingers; in particular $m \leq 4$ if K is two-dimensional.
(b) If, in addition, Σ is not an exceptional surface then
  (a) K can be held with a force/torque closure grasp by a positive grip of $m \leq 2k$ fingers; in particular $m \leq 6$ if K is two-dimensional.
  (b) Any external force/torque $\underline{e} = [\underline{F}, \underline{\tau}]$ acting on K can be balanced by a positive grip of $m \leq k$ fingers; in particular, $m \leq 3$ if K is two-dimensional.

The proof of the above theorem is given in Appendix A.

4.2. Physical analogy between grasping and lateral undulation

We now return to our own system. We already mentioned that the articulated mechanism *Snaca-N* could be instantaneously considered as a rigid body. This is the starting point of the analogy between grasping and lateral undulation. Fig. 9 illustrates an instantaneous configuration of the *Snaca-5* in motion.

The mechanisms whose links are drawn by solid lines and whose links are drawn by pointed lines represent, respectively, the actual and desired configurations of *Snaca-5*. Let $\underline{e} = [e_x\ e_y\ e_\theta]$ be the position error of the mass centre G and the global orientation of the mechanism with respect to a desired trajectory. This error must be compensated by an exterior force/torque $\underline{\Gamma} = [\underline{F}, \underline{\tau}]$, to be applied to the mechanism through discrete push-points.

We know by far that lateral contact forces are «propulsive» for *Snaca-N*. The desired motion of the mechanism depends on the generation of desired lateral forces. The position (and orientation) error $\underline{e}$ is arbitrary and the total exterior force/torque $\underline{\Gamma}$ necessary to correct it must be distributed to discrete push-points.

The contact forces of *Snaca-N* correspond to gripping forces generated for grasping an object. Taking into account the definition of the force/torque closure grasp, the physical analogy between the two phenomena is resumed in Table I.

We now propose the following theorem inspired by the above presented analogy, which will serve as a controllability criterion for *Snaca-N* to exert the lateral undulation.

Table I. Physical analogy between grasping and lateral undulation.

	Grasping	Limbless locomotion by lateral ondulation
Mobile body	Gripped object	Snaca-N
Exterior force/ torque in order to . . .	. . . stabilize the gripped object	. . . propulse the Snaca-N

Assumption 4. Each link can be positioned accurately, subject to only a small deviation due to a lumped compliance between top and bottom of the push-point.

Assumption 5. The mobile mechanism is a closed bounded connected domain in two-dimensional space and has a piecewise smooth boundary Σ.

Assumption 6. At each link/push-point contact can occur only a single pure force, normal to link's lateral faces through a frictionless point contact.

Theorem 2. Let *Snaca-N* be the planar mechanism defined in section 3 (Fig. 6), where it satisfies the above assumptions 4, 5 and 6, in an arbitrary initial configuration with respect to its environment. Let m be the number of simultaneous contacts at this initial moment. Then *Snaca-N* can be controlled to exert lateral undulation if $m \leq 6$.

In other words, the number 6 corresponds to the simultaneously necessary lateral contacts to control *Snaca-N* in any arbitrary configuration. We know by observation that the minimal number of simultaneous contacts for a snake to exercise the lateral undulation is 3. The difference is due to different contact properties in each case. *Snaca-N* is a simplified snake model interacting with the environment through frictionless point contacts. On the other hand, snakes in their natural environment establish surface contacts with friction.

An interesting approach to locomotion applications by considering analogies with grasping can be found in the reference.[32] In the next section, we present some results of dynamic simulations validating our controllability criterion.

https://doi.org/10.1017/S0263574704000244 Published online by Cambridge University Press

5. DYNAMIC SIMULATIONS OF THE CONTROLLED MECHANISM

Dynamic motion simulations of *Snaca-N*, which are realized by using various numbers of links and simultaneous push-points during one progression step, have been achieved in arbitrarily chosen different initial configurations. Link/Push-point interactions are represented by surface *versus* sphere contacts in order to obtain point contacts.

Let $\underline{\Psi}_0$ and $\underline{\Psi}_1$ be the arbitrarily chosen initial and final configurations of *Snaca-N* for a progression step and $P_i, i = 1, \ldots, m$ be the m push-points disposed in given proximities of m links of *Snaca-N*. We assume that at the initial moment, the considered m links are in simple contact with the push-points, i.e. they touch them without applying any force. The trajectory to be followed by the mechanism is the line segment joining the initial (G_0) and final (G_1) positions of the mass centre. To each point of this line segment corresponds one state of the mechanism in terms of positions.

Reconsidering *Snaca-N* instantaneously as a rigid body (Fig. 9), one needs to correct the position and orientation errors represented by $\underline{e} = \lfloor e_x \; e_y \; e_\theta \rfloor$ at each integration step of the simulation. The amplitude of the required total force is determined by feedbacking the system's linear velocity through a proportional gain:

$$\underline{F} = k_{P_1} \cdot (|\underline{v}_d| - |\underline{v}|) \tag{6}$$

where k_{P_1} is the proportional gain, $\underline{v}_d$ the desired velocity and $\underline{v}$ the actual velocity. Direction of the desired total force is determined by the vector $\underline{G_a G_d}$, G_a and G_d being the actual and desired positions of the mechanism's mass centre. The required torque is also given by a similar feedback on the mechanism's angular velocity:

$$\underline{\tau} = k_{P_2} \cdot (\underline{\omega}_d - \underline{\omega}) \tag{7}$$

where k_{P_2} is the proportional gain, $\underline{\omega}_d$ the desired angular velocity and $\underline{\omega}$ the actual angular velocity.

Once the required total force and torque are determined, one needs to distribute them to discrete contacts. Equations relating desired lateral forces to the system's geometric constraints are indicated below:

$$\begin{cases} F_1 \cdot \cos\gamma_1 + F_2 \cdot \cos\gamma_2 + \cdots + F_n \cdot \cos\gamma_n = -F_x \\ F_1 \cdot \sin\gamma_1 + F_2 \cdot \sin\gamma_2 + \cdots + F_n \cdot \sin\gamma_n = -F_y \\ F_1 \cdot (GP_{1x} \cdot \sin\gamma_1 - GP_{1y} \cdot \cos\gamma_1) + \cdots + F_n \\ \quad \cdot (GP_{nx} \cdot \sin\gamma_n - GP_{ny} \cdot \cos\gamma_n) = -\tau \end{cases} \tag{8}$$

$$F_i \geq 0, \quad i = 0 \ldots n \tag{9}$$

Equations (8) are the equalities representing the total force and torque projected to orthogonal $O - xyz$ axes in presence of n simultaneous lateral contacts. GP_i represent the distances between the system's mass centre and the lateral contacts and γ_i the orientations of the interacting links with respect to a reference frame. Inequalities (9) translate the fact that desired lateral forces are unilateral.

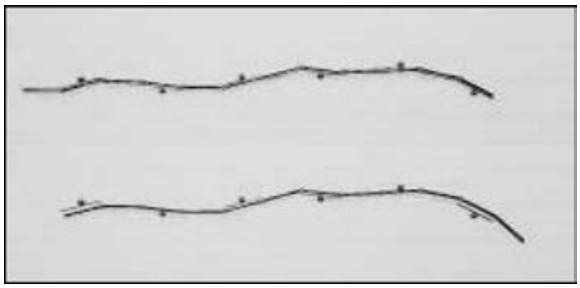


Fig. 10. Initial and final configurations of the Snaca-12.

Table II. Simulation parameters of the Snaca-12 in the Fig. 11.

Total mass	1,076 kg
Friction coefficient (with the ground)	0,3
Mechanism's desired velocity	0,3 m/s
Displacement of the mass centre	0,130 m
Length of a progression step	0,685 s

In the above system of equations (8) and (9), there are 3 equalities and n inequalities for n unknown variables. The n desired lateral forces at each integration step are obtained through a nonlinear constrained optimization algorithm (by quadratic computation) which is called at each (integration) step. This computation corresponds to the distribution of the required total propulsive force to discrete push-points. During its motion, the mechanism happens to be in a number of arbitrarily different configurations with respect to the fixed push-points. In order for the motion to be maintained, the optimization algorithm has to return a solution concerning the distribution of the desired propulsive force at each integration step. Hence this optimization is the key process of the present work.

A dynamic simulation software (Working Model ®) is used for the integration of motion equations. The above mentioned optimization is realized with a nonlinear constrained optimization algorithm by a successive quadratic programming technique. A numerical computation software (O-Matrix ®) is used in this end. The simulation setup under Windows 98 ® operating system is presented in Appendix C.

In Fig. 10 an example of initial and final configurations of the Snaca-12 moved along one progression step is shown. Global parameters of this step are given in Table II.

In Figs. 11 and 12, we present respectively the lateral forces created at two simultaneous contacts among others. One can observe that at the moments of link transitions (when one link looses its contact with a push-point and its following link establishes the contact with the same push-point), a certain continuity of lateral force is maintained. On the other hand, oscillations due to the link/push-point impacts during link transitions are present on the curves. We remark that these perturbations do not affect the global desired motion.

Several simulations have been achieved under the above defined conditions. Examples of initial and final configurations of *Snaca-N* pushing simultaneously against 3 and 4 push-points are given in Appendix B.

https://doi.org/10.1017/S0263574704000244 Published online by Cambridge University Press

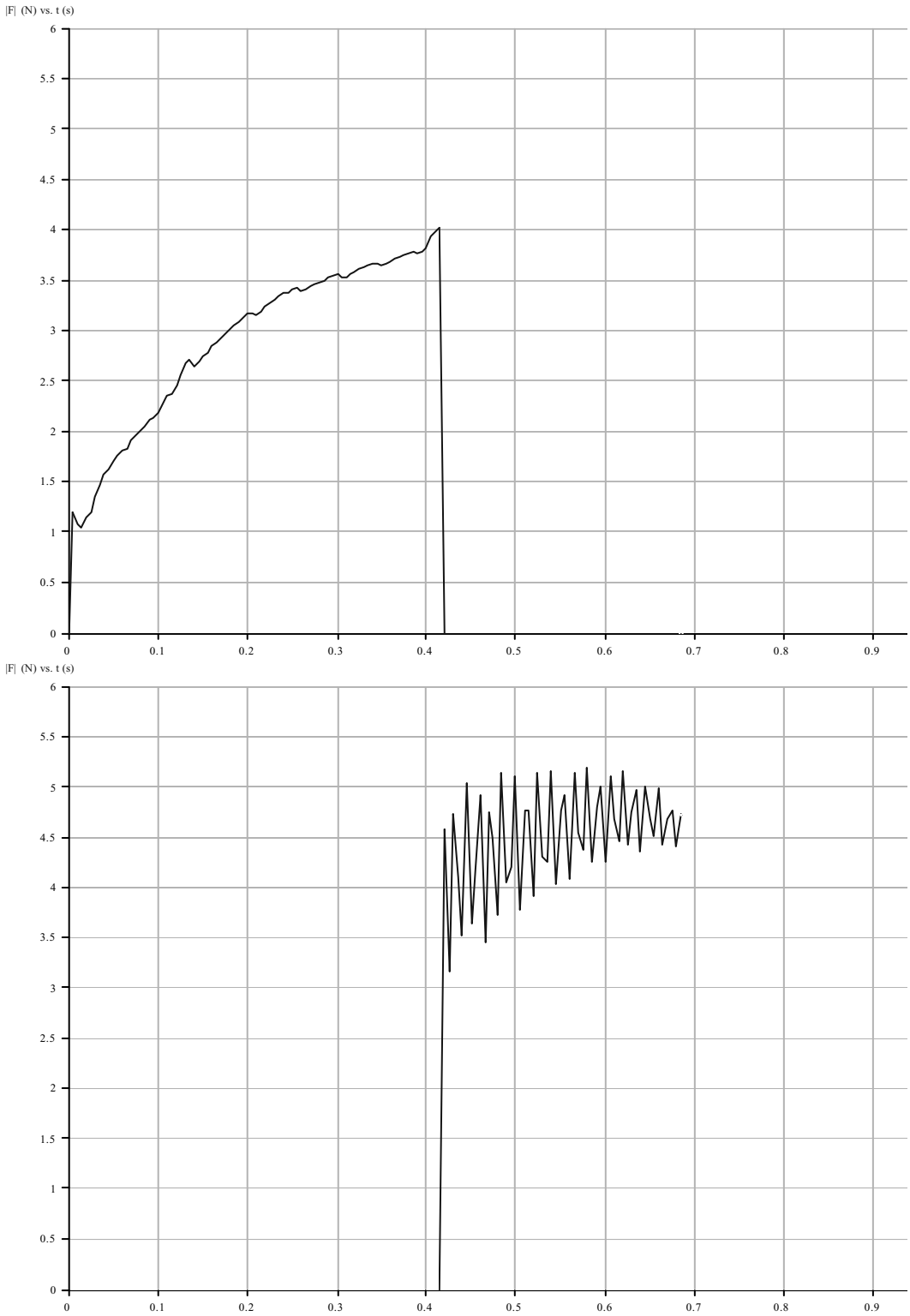


Fig. 11. Lateral force created at third of the link/push-point contacts, (F(N) versus t(s)).

Finally, our observation on the controllability of *Snaca-N* for its progressive motion by lateral undulation is as follows:

- When simultaneously pushing against 6 push-points, i.e. $m = 6$, the mechanism systematically achieves its progression step, independently from the initial configuration and the number of links, i.e. DOFs of the mechanism.
- On the other hand, when the number of simultaneously contacted push-points is less then 6, i.e. $m < 6$, the motion happens to be interrupted by the optimization algorithm which fails to return solutions to the problem of force distribution. In other words, when $m < 6$, the required force distribution is not guaranteed and therefore nor is the progression by lateral undulation.

https://doi.org/10.1017/S0263574704000244 Published online by Cambridge University Press

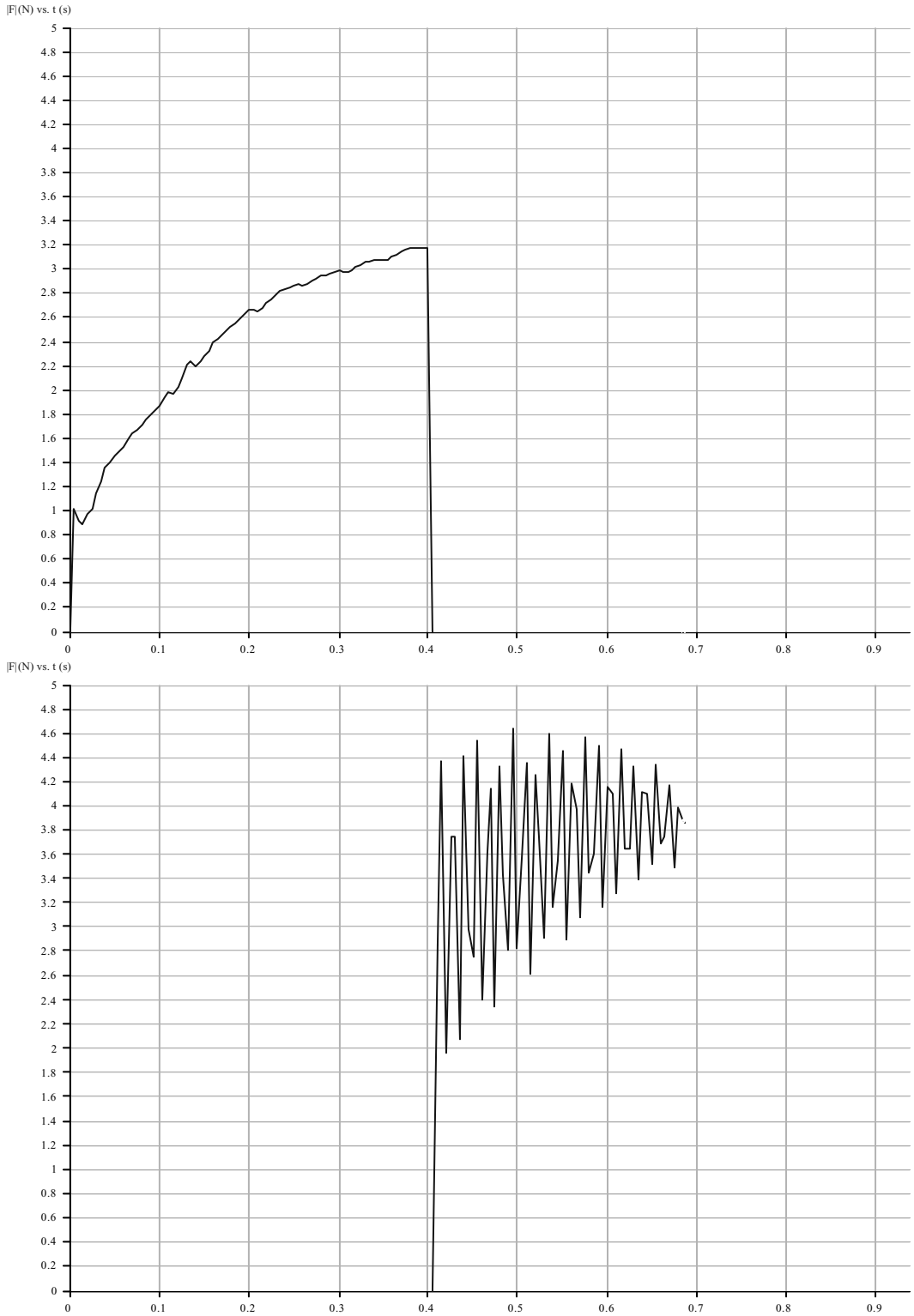


Fig. 12. Lateral force created at sixth of the link/push-point contacts, (F(N) versus t(s)).

6. CONCLUSION

Simulation results point to a systematic behavior which validates our analogy-based controllability criterion. Examples given in Appendix B are among the special initial configurations where the progression step is achieved despite a number of simultaneous lateral contacts less than 6. This analogy between limbless locomotion by lateral undulation and grasping is reconsidered in our ongoing study concerning the controllability of snake-like mechanisms interacting through surface contact with friction.

On the other hand, the analogy established between two different research fields within robotics reveals an example for the existence of basic physical features common to mechanical systems whose similarities are not necessarily obvious in appearance.

https://doi.org/10.1017/S0263574704000244 Published online by Cambridge University Press

References

1. Z. Y. Bayraktaroglu, "Locomotion apode: Application à la robotique mobile avec un mécanisme de type serpent", *Ph.D. Thesis* (University of Versailles, Versailles, France, 2002).
2. Z. Y. Bayraktaroglu, F. Butel, V. Pasqui and P. Blazevic, "Snake-like locomotion: Integration of geometry and kineto-statics", *Advanced Robotics* **14**(6), 447–458 (2000).
3. J. Gray, "The Mechanism of Locomotion in Snakes", *J. of Experimental Biology* **23**(2), 101–120 (1946).
4. J. Gray, *How Animals Move* (Cambridge University Press, 1960).
5. B. C. Jayne, "Kinematics of Terrestrial Snake Locomotion", *Copeia* **4**, 915–927 (1986).
6. A. R. McNeill, *Exploring Biomechanics: Animals in Motion* (Scientific American Library, 1992).
7. J.-P. Gasc, "Biology of Snakes: Locomotion", **In**: (R. Bauchot Ed), *Snakes: A natural History* (Translated in English by C. Berthier, Streling Publishing Co., Inc., New York, 1994) pp. 60–75.
8. S. Renous, *Locomotion* (Dunod, Paris, 1994).
9. K. C. Kelley, S. J. Arnold and J. Gladstone, "The Effects of Substrate and Vertebral Number on Locomotion in Garter Snake Thamnophis Elegans", *Functional Ecology* **11**, 189–198 (1997).
10. S. Hirose, *Biologically Inspired Robots/Snake-like Locomotors and Manipulators* (Translated into English by P. Cave and C. Goulden, Oxford University Press, 1993).
11. M. Mori and S. Hirose, "Development of Active Chord Mechanism ACM-R3 with Agile 3D Mobility", *Proc. IEEE/RSJ IROS'01*, Maui, HA (2001) pp. 1552–1557.
12. J. W. Burdick, J. Radford and G. S. Chirikjian, "A Sidewinding Locomotion Gait for Hyper-Redundant Robots", *Advanced Robotics*, **9**(3), 195–216 (1995).
13. G. S. Chirikjian, "Theory and Applications of Hyper-Redundant Robotic Manipulators", *Ph.D. Thesis* (CalTech, Pasadena, CA, 1992).
14. G. S. Chirikjian, "Hyper-redundant Manipulator Dynamics: A Continuum Approximation", *Advanced Robotics* **9**(3), 217–244 (1995).
15. G. S. Chirikjian and J. W. Burdick, "Design and Experiments with a 30 Degree-of-Freedom Hyper-redundant Robot", *Proc. IEEE/ICRA'93*, Atlanta, GA (1993) **Vol. 3**, pp. 113–119.
16. J. P. Ostrowski, "Geometric Perspectives on the Mechanics and the Control of Undulatory Robotic Locomotion", *Ph.D. Thesis* (CalTech, Pasadena, CA, 1995).
17. K. J. Dowling, "Limbless Locomotion: Learning to Crawl with a Snake Robot", *Ph.D. Thesis* (CMU, Pittsburgh, PA, 1997).
18. B. Klaassen and K. L. Paap, "GMD-SNAKE 2: A Snake-like Robot Driven by Wheels and a Method for Motion Control", *Proc. IEEE/ICRA'99* Detroit, MI (1999) pp. 3014–3019.
19. G. Miller, "Snake Robots for Search and Rescue", **In**: (J. Ayers, J. L. Davis and A. Rudolph, Eds.), *Neurotechnology for Biomimetic Robots* (The MIT Press, Cambridge, Massachusetts, 2002) pp. 271–284.
20. J. I. Neimark and N. A. Fufaev, *Dynamics of Nonholonomic Systems* (Translated into English by J. R. Barbour, Translations of mathematical monographs 33, American Mathematical Society, Providence RI, 1972).
21. N. Sreenath, "Modeling and Control of Multibody Systems", *Ph.D. Thesis* (University of Maryland, MD, 1987).
22. N. Sreenath, Y. G. Oh, P. S. Krishnaprasad and J. E. Marsden, "The Dynamics of Coupled Rigid Bodies; Part I: Reduction, Equilibria and Stability", *Dynamics and Stability of Systems* **3**(1,2), 25–49 (1988).
23. M. Reyhanoglu and N. H. McClamroch, "Controllability and Stabilizability of Planar Multibody Systems with Angular Momentum Preserving Control Torques", *Proc. American Control Conference*, Boston (1991) pp. 1102–1107.
24. M. Reyhanoglu and N. H. McClamroch, "Planar Reorientation Maneuvers of Space Multibody Systems Using Internal Controls", *J. of Guidance, Control and Dynamics* **15**(6), 1475–1480 (1992).
25. M. Reyhanoglu and N. H. McClamroch, "Nonlinear Attitude Control of Planar Structures in Space Using Only Internal Controls", *Fields Institute Communications* **2**, 91–100 (1993).
26. R. Yang, "Nonholonomic Geometry, Mechanics and Control", *Ph.D. Thesis* (University of Maryland, MD, 1992).
27. A. De Luca and G. Oriolo, "Modelling and Control of Nonholonomic Mechanical Systems", In: (J. Angeles and A. Kecskeméthy, Eds.), *Kinematics and Dynamics of Multi-Body Systems* (CISM Courses and Lectures No. 360, Springer-Verlag, 1995) pp. 277–342.
28. C. Gans, "Terrestrial Locomotion without Limbs", *American Zoologist* **2**, 167–182 (1962).
29. B. Mishra, J. T. Schwartz and M. Sharir, "On the Existence and Synthesis of Multifinger Positive Grips", *Algorithmica* **2**(4), 541–558 (1987).
30. E. Rimon and J. W. Burdick, "New Bounds on the Number of Frictionless Fingers Required to Immobilize Planar Objects", *J. of Robotic Systems* **12**(6), 433–451 (1995).
31. E. Rimon and J. W. Burdick, "On Force and Form Closure For Multiple Finger Grasps", *Proc. IEEE/ICRA'96* St. Paul, MN (1996) pp. 1795–1800.
32. G. S. Chirikjian and J. W. Burdick, "Kinematics of Hyper-redundant Robot Locomotion", *IEEE Trans. on Robotics & Automation* **11**, 781–793 (1995).
33. C. Carathéodory, "Uber den Variabilitatsbereich der Koeffizienten von Potenzreihen, die gegebene Werte nicht annehmen", *Math. Ann.* **64**, 95–115 (1907).
34. L. Danzer, B. Grunbaum and V. Klee, "Helly's Theorem and its Relatives", *Proc. Symposia in Pure Maths* (1962) **7** (Convexity) pp. 433–451.
35. E. Steinitz, "Bedingt Konvergente Reihen und Konvexe Systeme I", *J. reine angew. Math* **143**, 128–175 (1913).
36. E. Steinitz, "Bedingt Konvergente Reihen und Konvexe Systeme II", *J. reine angew. Math* **144**, 1–40 (1914).
37. E. Steinitz, "Bedingt Konvergente Reihen und Konvexe Systeme III", *J. reine angew. Math* **146**, 1–52 (1916).

APPENDIX A Proof of the existence theorem[29]

Lemma A.1. Let Σ be the boundary of an object K satisfying the assumptions 1, 2 and 3. Then

1. The origin O lies in the convex-hull of $\Gamma(\Sigma)$.
2. If, in addition, Σ is not an exceptional surface then the origin O lies in the interior of the convex-hull of $\Gamma(\Sigma)$.

Proof. It suffices to show that

$$\left[\int_\Sigma n(r)\,dS, \int_\Sigma (r \times n(r))\,dS\right] = 0. \qquad \text{(A.1)}$$

For each constant vector c, we have

$$c \cdot \int_\Sigma n\,dS = \int_\Sigma c \cdot n(r)\,dS = \int_K (div\, c)\,dV = 0 \qquad \text{(A.2)}$$

by Gauss' divergence theorem, showing that $\int_\Sigma n\,dS = 0$. Similarly, for each constant vector c, we have

$$c \cdot \int_\Sigma r \times n\,dS = \int_\Sigma n \cdot (c \times r)\,dS = \int_K div(c \times r)\,dV. \qquad \text{(A.3)}$$

But $div(c \times r) = 0$. Therefore $\int_\Sigma r \times n\,dS = 0$, as claimed.

https://doi.org/10.1017/S0263574704000244 Published online by Cambridge University Press

The following two classical theorems are stated without proof; the reader may consult the indicated references for their proofs.

Theorem A.1 Carathéodory's theorem[33,34]. If $X \subseteq \mathbb{R}^n$ and $p \in \text{ConvexHull}(X)$, then $p \in \text{ConvexHull}(Y)$ for some $Y \subseteq X$ with $|Y| \leq n+1$.

Theorem A.2 Steinitz's theorem[34–37]. If $X \subseteq \mathbb{R}^n$ and $p \in \text{Interior}(\text{ConvexHull}(X))$, then $p \in \text{Interior}(\text{ConvexHull}(Y))$ for some $Y \subseteq X$ with $|Y| \leq 2n$.

Proof of the Existence Theorem
By the Lemma A.1, the origin lies in the convex hull of $\Gamma(\Sigma)$, i.e.

$$0 \in \text{ConvexHull}(\Gamma(\Sigma)).$$

Carathéodory's Theorem implies that

$$0 \in \text{ConvexHull}(Y),$$

for some $Y = \{\Gamma(r_1), \ldots, \Gamma(r_m)\} \subseteq \Gamma(\Sigma)$, and $m \leq k+1$. If K is two-dimensional, then $\Gamma(\Sigma) \subseteq \mathbb{R}^6$ and $m \leq 7$.

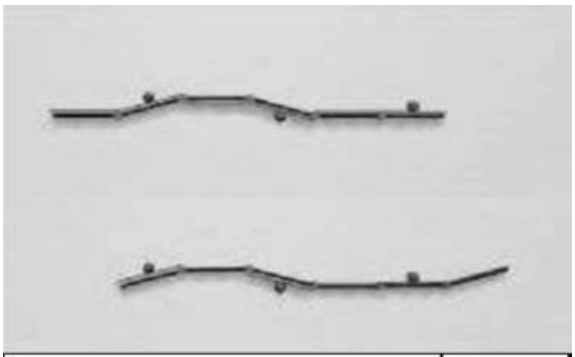
Hence there exist positive real quantities $\alpha_1, \ldots, \alpha_m$ with $\alpha_1 + \ldots + \alpha_m = 1$ such that

$$\alpha_1 \Gamma(r_1) + \ldots + \alpha_m \Gamma(r_m) = 0. \qquad \text{(A.4)}$$

The positive grip consists of the grip points $\{r_1, \ldots, r_m\}$ and the force targets $\{\alpha_1, \ldots, \alpha_m\}$.

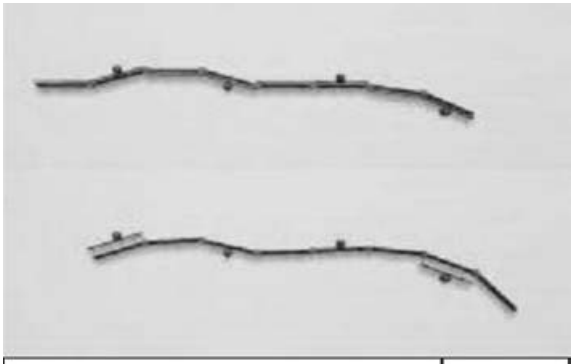
APPENDIX B Examples of Simulation Results

Initial and final configurations of Snaca-N in one progression step are shown in Figs. 13 to 15.



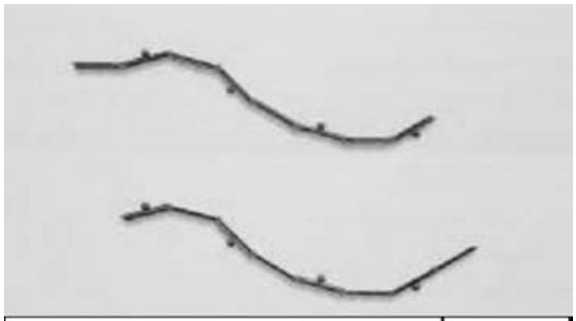
Total mass	0,535 kg
Friction coefficient (with the ground)	0,3
Mechanism's desired velocity	0,3 m/s
Displacement of the mass centre	0,131 m
Length of a progression	0,48 s

Fig. 13. Initial and final configurations of the Snaca-6 pushing simultaneously against 3 push-points.



Total mass	0,716 kg
Friction coefficient (with the ground)	0,3
Mechanism's desired velocity	0,3 m/s
Displacement of the mass centre	0,130 m
Length of a progression step	0,985 s

Fig. 14. Initial and final configurations of the Snaca-8 pushing simultaneously against 4 push-points, first example.



Total mass	0,716 kg
Friction coefficient (with the ground)	0,3
Mechanism's desired velocity	0,3 m/s
Displacement of the mass centre	0,123 m
Length of a progression step	0,495 s

Fig. 15. Initial and final configurations of the Snaca-8 pushing simultaneously against 4 push-points, second example.

APPENDIX C Simulation tools

Dynamic simulation of the controlled mechanism is realized in a modular computing environment where three softwares cooperate under MS Windows 98 ®.

In the central module, Borland C++ Builder ® (version 4), is compiled a $C/C++$ source code, which communicates with WorkingModel 4D ® (version 6.0) and O-Matrix ® (version 5.0). The first one simulates the dynamic behavior of the system and the second one is used for various optimizations.

Data transfers between the Builder and the WorkingModel is achieved through *OLE Automation* and between the Builder and the O-Matrix through *DDE*, which are the

https://doi.org/10.1017/S0263574704000244 Published online by Cambridge University Press

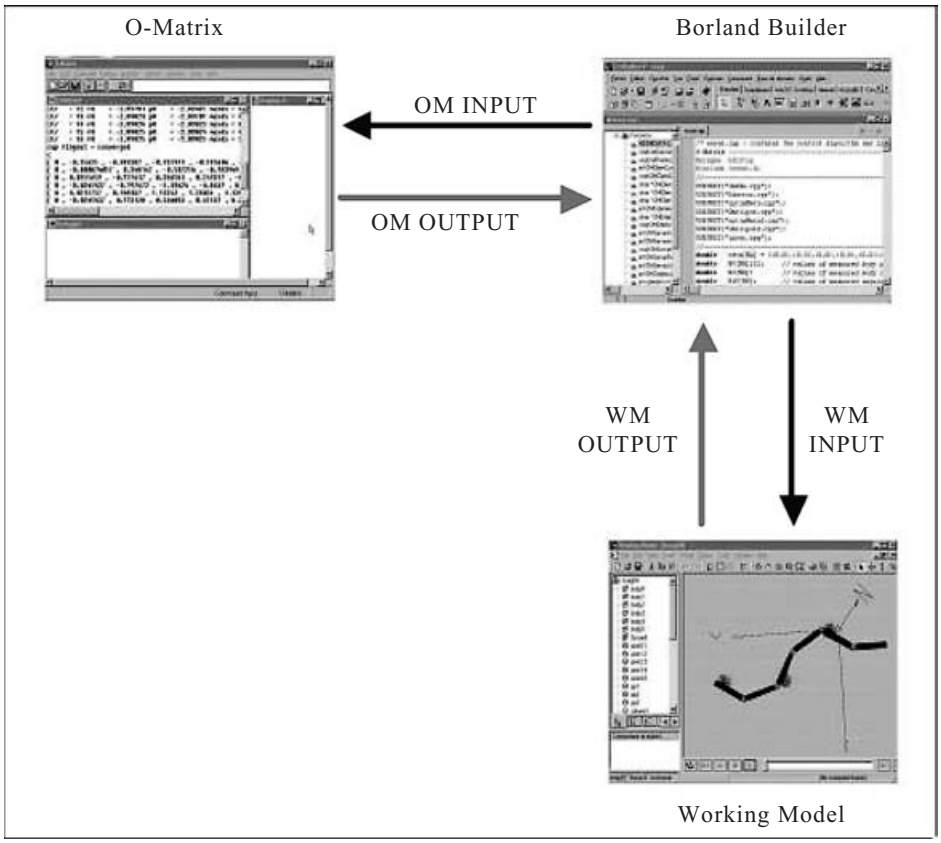


Fig. 16. Organization scheme of used softwares, with OM for O-Matrix and WM for Working Model.

Windows standard communication functions. Fig. 16 illustrates the organization scheme under Windows.

O-Matrix is a numerical computation software used particularly for its optimization functions such as the nonlinear constrained optimization function by successive quadratic programming technique.

The *C*/*C*++ source code compiled in Borland Builder contains the system's main control loop. Dynamic parameters such as the inertia matrices and the matrices of centrifugal and Coriolis forces are computed through integrated functions. Decisions on control laws are determined in the Borland Builder and pure control inputs are sent to the Working Model, which simulates the dynamic behavior of the mechanism and returns required measurements at the end of each integration step to the Borland Builder.

https://doi.org/10.1017/S0263574704000244 Published online by Cambridge University Press